Electronic Supplementary Material (ESI) for Journal of Materials Chemistry B.

Supplementary Information

Gold nanoparticles impair autophagy flux through shape-dependent endocytosis and lysosomal dysfunction

Hualu Zhou,[a,‡] Xuanqing Gong,[a,‡] Hongyu Lin,[a,‡] Hongming Chen,[a] Dengtong Huang,[a] Dan Li,[b] Hong Shan,[b,*] and Jinhao Gao[a,*]

[a] State Key Laboratory of Physical Chemistry of Solid Surfaces, The MOE Key Laboratory of Spectrochemical Analysis & Instrumentation, The Key Laboratory for Chemical Biology of Fujian Province, and Department of Chemical Biology, College of Chemistry and Chemical Engineering, Xiamen University, Xiamen 361005, China.

[b] Department of Interventional Medicine, Guangdong Provincial Engineering Research Center of Molecular Imaging ,The Fifth Affiliated Hospital, Sun Yat-sen University, Zhuhai 519000, China.

‡These authors contributed equally to this work.

*E-mail: shanhong@mail.sysu.edu.cn, jhgao@xmu.edu.cn

Table S1. Morphology Size and zeta-potential of gold nanoparticles.

Sample	Shape	Length (nm)	Width (nm)	Volume ($\times 10^3$ nm^3)	Zeta-potential (mV)
Au-20 Sphere	Sphere	20.1±1.6 (diameter)		4.35±1.05	-23.3
Au-50 Sphere	Sphere	49.4±6.7 (diameter)		66.9±26.1	-29.3
Au-40 Rod	Rod	37.5±3.0	11.6±1.4	5.26±1.67	-20.6
Au-90 Rod	Rod	89.3±5.8	24.6±2.0	54.9±12.1	-31.1
Au-20 Sphere@ PEG	Sphere	21.4±2.4 (diameter)		4.10±1.54	-15.2
Au-40 Rod@ PEG	Rod	41.1±2.3	11.0±0.6	4.97±0.87	-16.1

The size of gold nanoparticles was measured from TEM images.

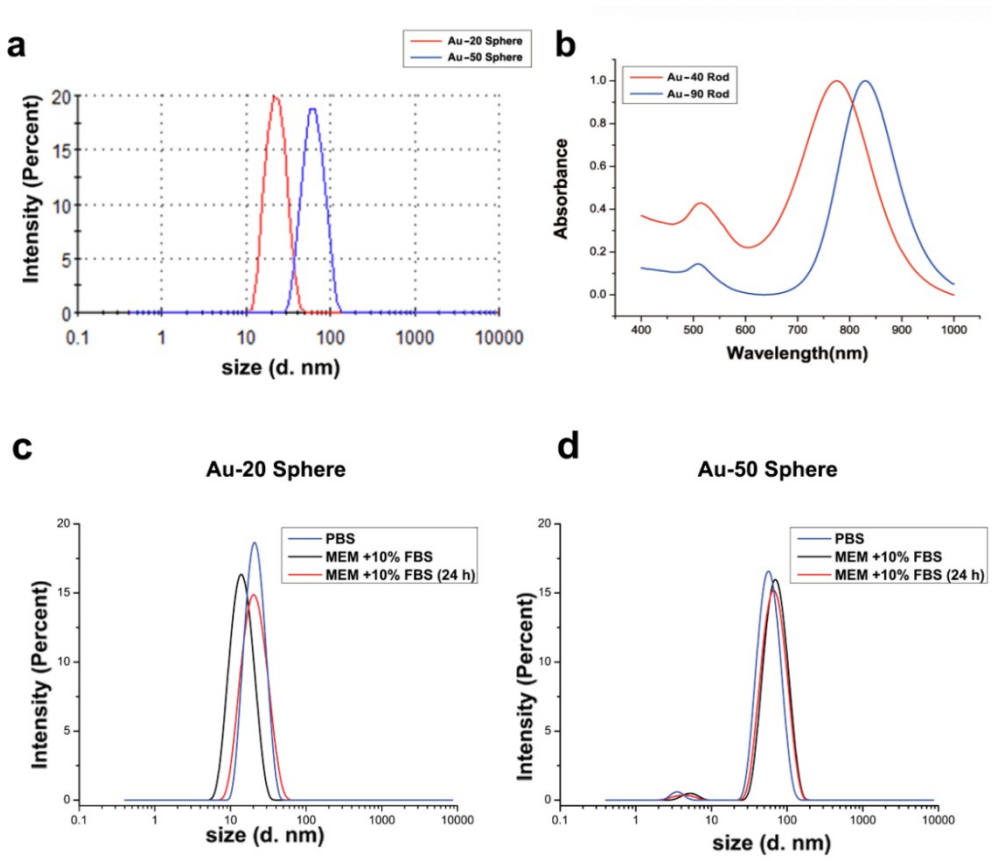

Figure S1. (a) Hydrodynamic diameters of Au-20 Sphere and Au-50 Sphere. (b) UV-vis-NIR spectra of Au-40 Rod and Au-90 Rod. (c) Stability of Au-20 Sphere in 10% serum-containing MEM. (d) Stability of Au-50 Sphere in 10% serum-containing medium.

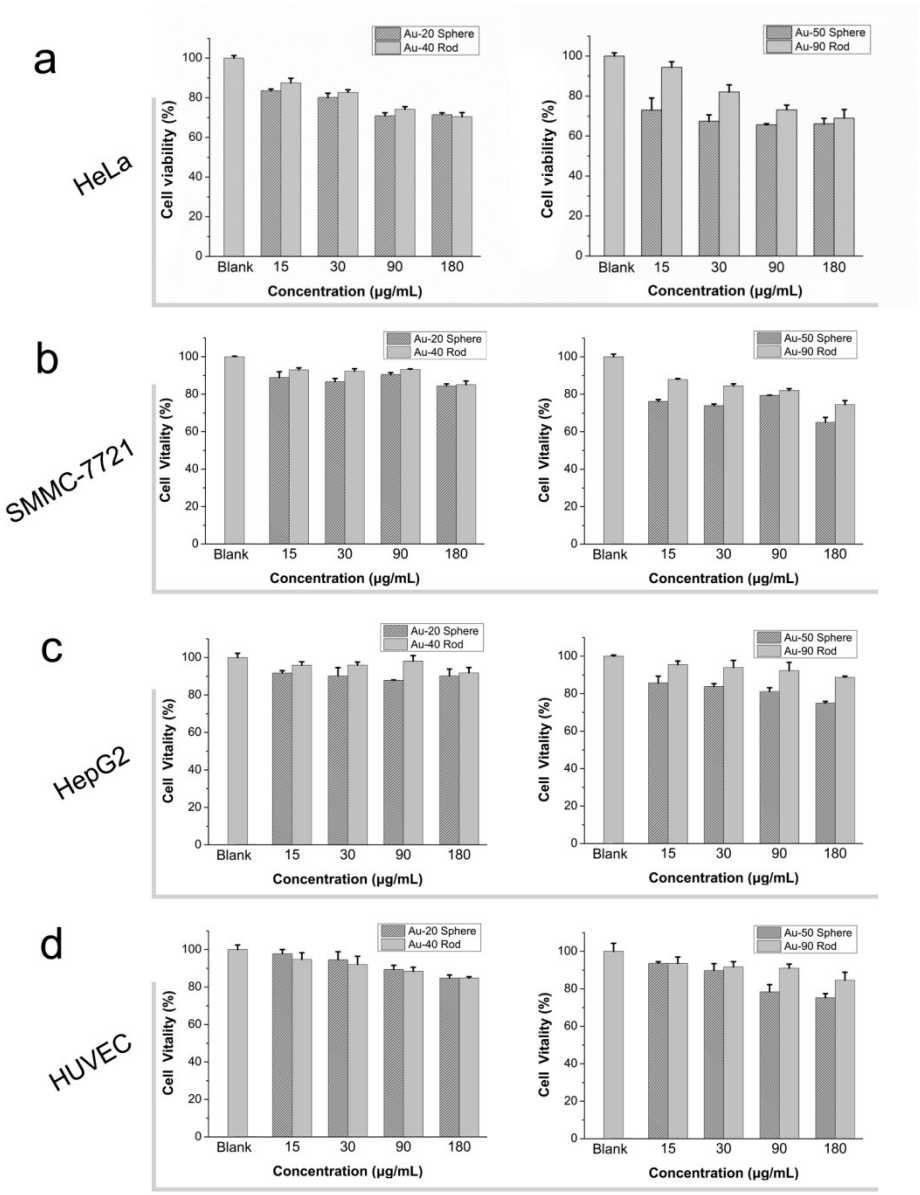

Figure S2. Cell viability of (a) HeLa, (b) SMMC-7721, (c) HepG2, and (d) HUVEC treated with Au-20 Sphere and Au-40 Rod nanoparticles (left column) and Au-50 Sphere and Au-90 Rod (right column). Cell viability was measured at 24 h by MTT assay. Data were presented as the average of three replicates with standard deviation.

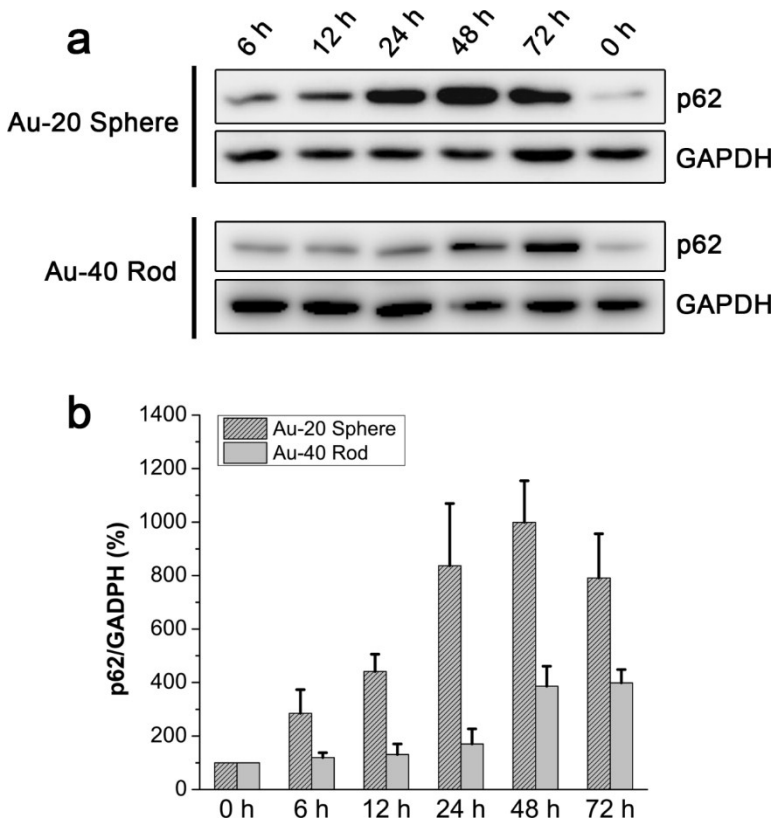

Figure S3. Time dependent accumulation of p62. (a) Western blot analysis of p62. Cells were treated with Au-20 Sphere and Au-40 Rod at 90 μg/mL for 6, 12, 24, 48, and 72 h. (b) The relative expression levels of p62 over GAPDH with the value of blank normalized to 100%. Data were mean ± SD, $n = 3$.

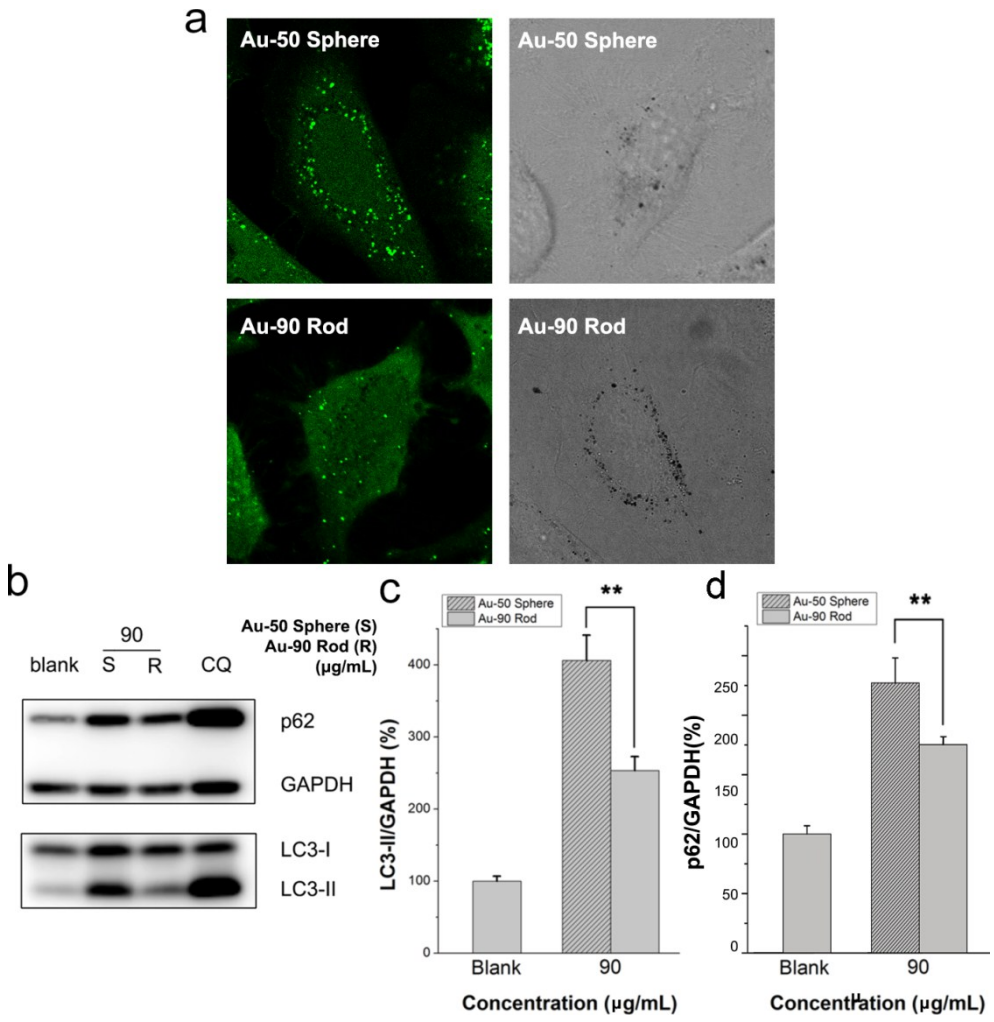

Figure S4. Effects of the shape of larger gold nanoparticles on autophagy. (a) The left views were fluorescent images taken by confocal microscope. The right views were bright field images. (b)Western blot analysis of autophagy related proteins. Cells were treated with Au-50 Sphere (S) and Au-90 Rod (R) at 90 μg/mL for 24 h. The relative expression levels of (c) LC3-II and (d) p62 over GAPDH with the value of blank normalized to 100%. Data were mean ± SD, $^{**}p < 0.01$, $n = 3$.

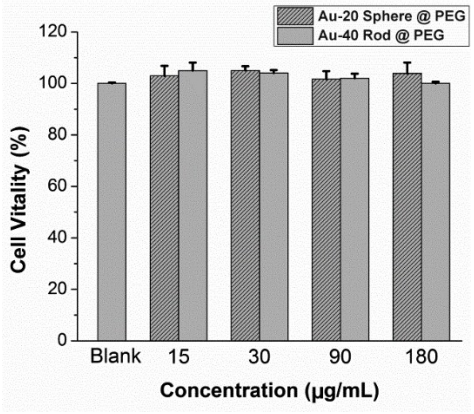

Figure S5. Cell vitality of HeLa cells treated with Au-20 Sphere @ PEG and Au-40 Rod @ PEG nanoparticles. Cell vitality was measured at 24 h by MTT assay. Data were presented as the average of three replicates with standard deviation.

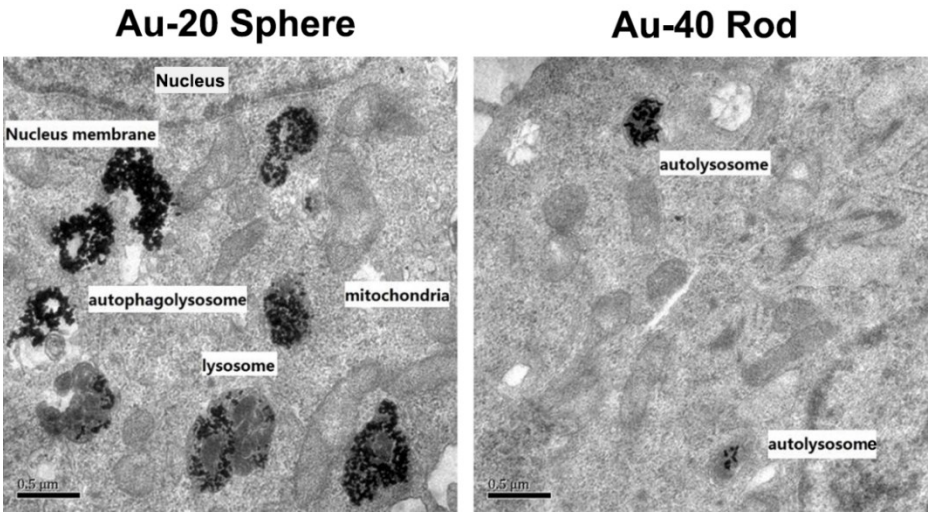

Figure S6. Autophagy-related organelles identified from TEM images. Cells were treated with Au-20 Sphere and Au-40 Rod at 90 μg/mL for 24 h.

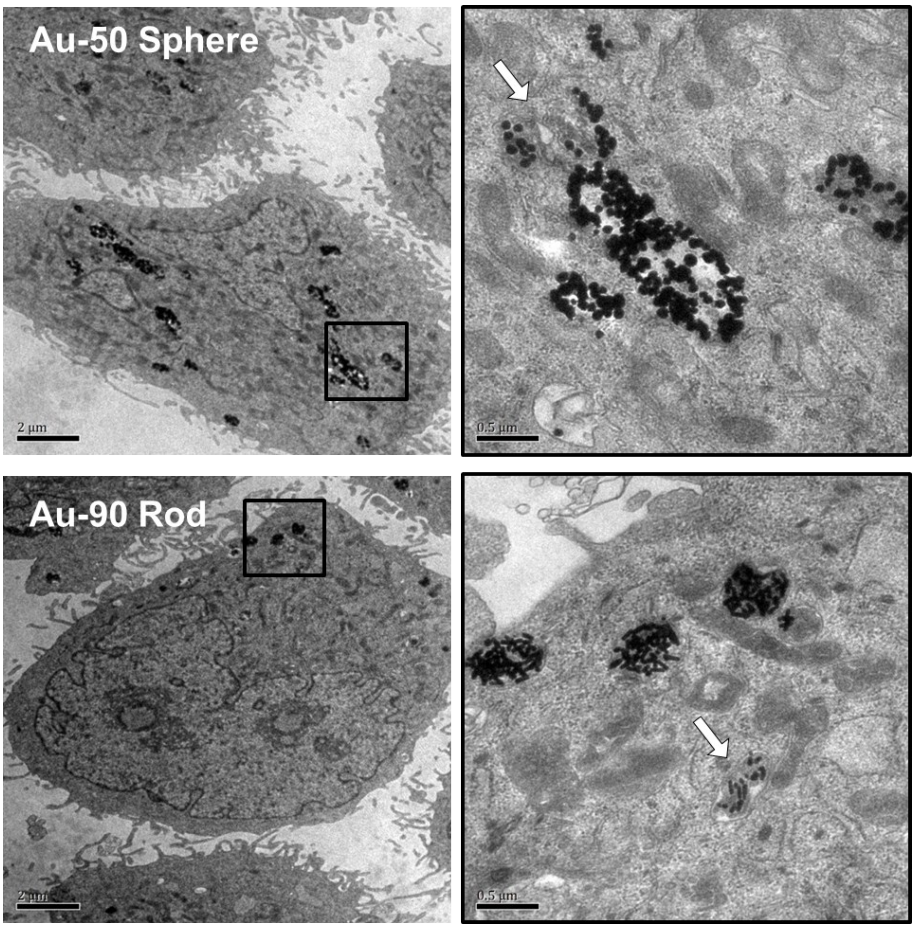

Figure S7. TEM images of cells after treated with Au-50 Sphere and Au-90 Rod for 24 h. The right views were the magnification of the regions inside the black boxes in the left views. White arrows indicated gold nanoparticles inside autolysosome.

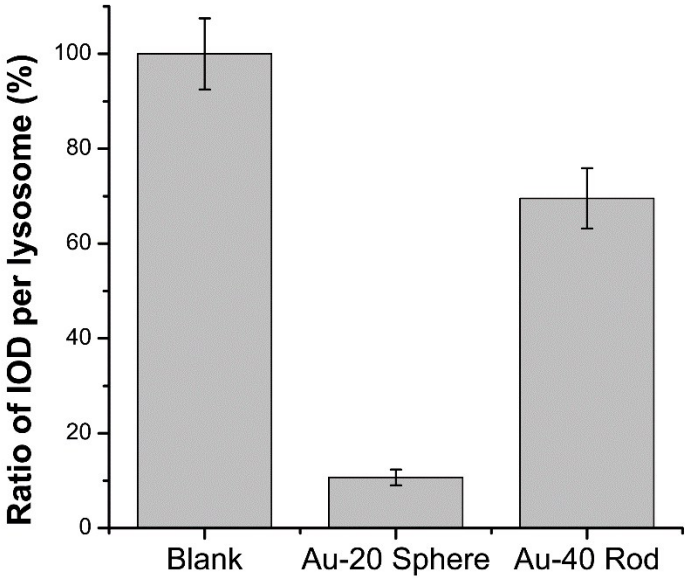

Figure S8. The normalized intensity of fluorescent puncta caused by lysosomal degradation (in Figure 7b) according to the amount of lysosomes per cell counted in TEM images. The results indicate a remarkable decrease of enzymatic activities after treatment with Au-20 Sphere while treatment with Au-40 Rod induces a slight decrease of enzymatic activities, which is consistent with Figure 7c.